Application of photoionization models based on radiative transfer and the Helmholtz equations to studies of streamers in weak electric fields

Ningyu Liu[a)]
Communications and Space Sciences Laboratory, Department of Electrical Engineering, The Pennsylvania State University, University Park, Pennsylvania 16802, USA

Sébastien Célestin[b)] and Anne Bourdon
Ecole Centrale Paris, EM2C, UPR CNRS 288, Grande voie des vignes, 92295 Châtenay-Malabry Cedex, France

Victor P. Pasko
Communications and Space Sciences Laboratory, Department of Electrical Engineering, The Pennsylvania State University, University Park, Pennsylvania 16802, USA

Pierre Ségur
Université de Toulouse, LAPLACE, CNRS, INPT, UPS, 118 route de Narbonne, 31062 Toulouse Cedex 9, France

Emmanuel Marode
Ecole Supérieure d'Electricité, LPGP, UMR CNRS 8578, Plateau du moulon, 3 rue Joliot Curie, 91192 Gif-sur-Yvette, France

(Received 14 September 2007; accepted 2 November 2007; published online 20 November 2007)

Recent advances in development of photoionization models in air based on radiative transfer and Helmholtz equations open new perspectives for efficient solution of nonthermal gas discharge problems involving complex geometries. Many practical applications require accurate modeling of streamer discharges developing in weak electric fields, in which the photoionization process significantly contributes to discharge dynamics. This paper (1) reports original studies, which demonstrate the validity and accuracy of the recently proposed photoionization models for studies of streamers in weak electric fields, and (2) introduces efficient boundary conditions for the photoinization models based on radiative transfer theory. © *2007 American Institute of Physics*. [DOI: 10.1063/1.2816906]

In a recent paper by Bourdon *et al.*[1] several models are discussed and developed for evaluation of photoionization produced by nonthermal gas discharges in air. In particular, the integral equation approach based on the model developed by Zheleznyak *et al.*[2] and two differential equation approaches based on the radiative transfer and Helmholtz equations, respectively, are investigated. For the Zheleznyak model, the photoionization rate at each observation point is calculated by conducting a three-dimensional (3D) integration over the region containing emission sources.[2,3] The Helmholtz model effectively replaces the calculation of the Zheleznyak integral with a solution of a set of Helmholtz differential equations.[4] A three-exponential Helmholtz model was developed in Ref. 1 for the purpose of streamer modeling. According to Ref. 5, the photoionization rate can be determined using the isotropic part of the photon distribution function. In Ref. 1, a three-group SP_3 model, based on the third order Eddington approximation of the radiative transfer equation, was found to be well suited for streamer simulations.

The work by Bourdon *et al.*[1] focused on the problem of streamer development in strong external electric fields ($>E_k$, the conventional breakdown threshold field defined by the equality of the electron impact ionization and electron dissociative attachment coefficients in air[6]). In the present paper, we introduce efficient boundary conditions for photoionization calculations based on radiative transfer theory and apply the three-exponential Helmholtz and three-group SP_3 models to the simulations of streamers propagating in weak external electric fields ($<E_k$), which is a regime of great interest for many practical applications of streamers. We validate the two models by comparing the corresponding results with those obtained with the Zheleznyak model. This work demonstrates the validity and accuracy of the three-exponential Helmholtz and three-group SP_3 models for studies of streamer discharges in air for a wide range of applied electric fields.

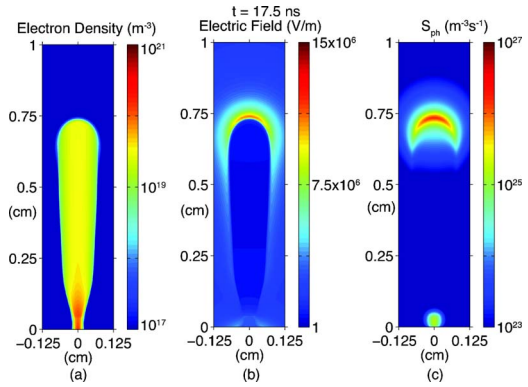

FIG. 1. (Color online) A cross-sectional view of distributions of (a) electron density, (b) electric field, and (c) photoionization production rate at $t=17.5$ ns calculated using the three-exponential Helmholtz model.

[a)]Electronic mail: nul105@psu.edu
[b)]Electronic mail: sebastien.celestin@em2c.ecp.fr

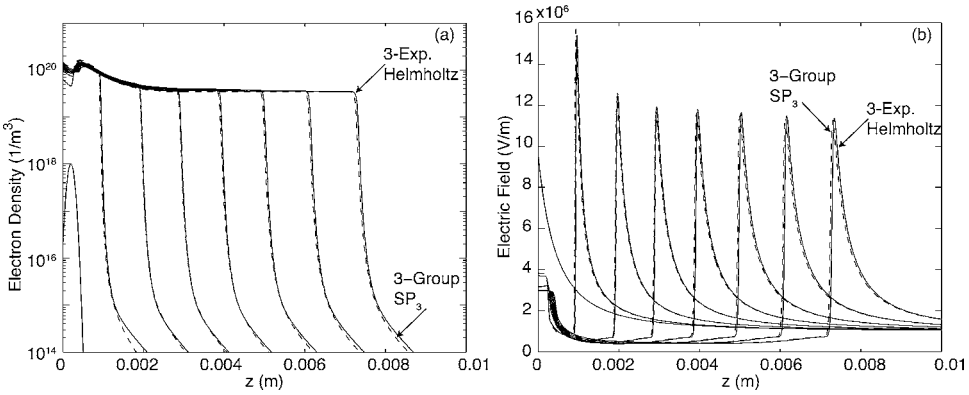

FIG. 2. Profiles of streamer characteristics along the symmetry axis of the computational domain at various moments of time calculated using different photoionization models. The results are obtained by the FCT based numerical technique (Ref. 1). (a) Electron density. (b) Electric field. Dashed line: three-group SP_3 with boundary conditions defined by Eqs. (1) and (2); Solid line: three-exponential Helmholtz model. Results are shown for the moments of time from $t=0$ to $t=17.5$ ns with a timestep of 2.5 ns.

The streamer model equations adopted in the present study consist of drift-diffusion equations for electrons and ions and Poisson's equation. We employ two sets of numerical techniques for solution of the streamer model equations: flux-corrected transport (FCT) method and a modified Scharfetter-Gummel (SG) algorithm. The boundary conditions for Poisson's equation are provided by the direct integral solution.[7] The boundary conditions for the Helmholtz model are provided by the Zheleznyak integral solution. Except where noted, the boundary conditions given by Eqs. (1) and (2) below are used for the SP_3 model. When using the Zheleznyak model, to optimize the computation of the 3D integral, an inhomogeneous grid with fine resolution around the streamer head and coarse resolution in the region away from the head is employed, and the emission source is assumed to be confined in the streamer head region. Details about the model equations, numerical algorithms, and computation acceleration techniques employed in our study can be found in Ref. 1.

We introduce efficient boundary conditions for the three-group SP_3 model. The third order Eddington approximation results in elliptic equations for functions $\phi^*_{1,j}(\mathbf{r})$ and $\phi^*_{2,j}(\mathbf{r})$, and a linear combination of $\phi^*_{1,j}(\mathbf{r})$ and $\phi^*_{2,j}(\mathbf{r})$ gives the isotropic part of the photon distribution function.[1,5] As derived in the work by Larsen *et al.*[8] for a boundary surface with no reflection and emission, the boundary conditions for $\phi^*_{1,j}$ and $\phi^*_{2,j}$ are given as

$$\nabla\phi^*_{1,j}(\mathbf{r})\cdot\mathbf{n}_s = -\lambda_j p_{O_2}\alpha_1\phi^*_{1,j}(\mathbf{r}) - \lambda_j p_{O_2}\beta_2\phi^*_{2,j}(\mathbf{r}), \qquad (1)$$

$$\nabla\phi^*_{2,j}(\mathbf{r})\cdot\mathbf{n}_s = -\lambda_j p_{O_2}\alpha_2\phi^*_{2,j}(\mathbf{r}) - \lambda_j p_{O_2}\beta_1\phi^*_{1,j}(\mathbf{r}), \qquad (2)$$

where $\mathbf{n}_s$ is the outward unit vector normal to the boundary surface, $\alpha_{1,2}=(5/96)(34\pm11\sqrt{6/5})$, and $\beta_{1,2}=(5/96)\times(2\mp\sqrt{6/5})$, where the upper and lower signs correspond to subscripts 1 and 2, respectively. The product $\lambda_j p_{O_2}$ is the absorption coefficient, where p_{O_2} is the partial pressure of molecular oxygen and the values of λ_j are given in Ref. 1. As for the coefficients $\alpha_{1,2} \gg \beta_{1,2}$, the coupling between both equations is weak. Following Ref. 8, the two equations are first solved independently and iterations are carried out afterward with the β coefficients. The convergence is very rapid and obtained in only a few iterations.

The geometry of the simulation domain is identical to the one employed by Liu and Pasko,[7] in which a small conducting sphere is placed in a weak uniform electric field E_0. The air pressure is fixed at a value of 760 Torr. The external homogeneous field E_0 is 10^6 V/m. The radius b and the potential applied to the conducting sphere Φ_0 are 0.1 cm and 6500 V, respectively. To initiate the development of a streamer, as a common practice, we place a cloud of plasma with spherically symmetric Gaussian spatial distribution on the axis of symmetry in the vicinity of the sphere, i.e., $n_e=n_p=n_0\exp\{-(r/\sigma_r)^2-[(z-z_0)/\sigma_z]^2\}$, where n_e and n_p are densities of electrons and positive ions, respectively, $n_0=10^{18}$ m^{-3}, $\sigma_r=\sigma_z=0.01$ cm, and $z_0=0.02$ cm. The size of the computational domain is 1.0×0.125 cm. The computational grid is uniform in both radial and axial directions. The numbers of grid points in axial and radial directions are 1601 and 201, respectively.

Figure 1 shows a cross-sectional view of the distributions of the electron density, electric field, and photoionization production rate at $t=17.5$ ns obtained using the three-exponential Helmholtz model. This cross-sectional view represents an example of two-dimensional views of simulation results obtained by using different photoionization models. The streamer expands as it propagates [Fig. 1(a)]. The photoionization production rate is maximized in the head region, and there is no significant contribution in the body of

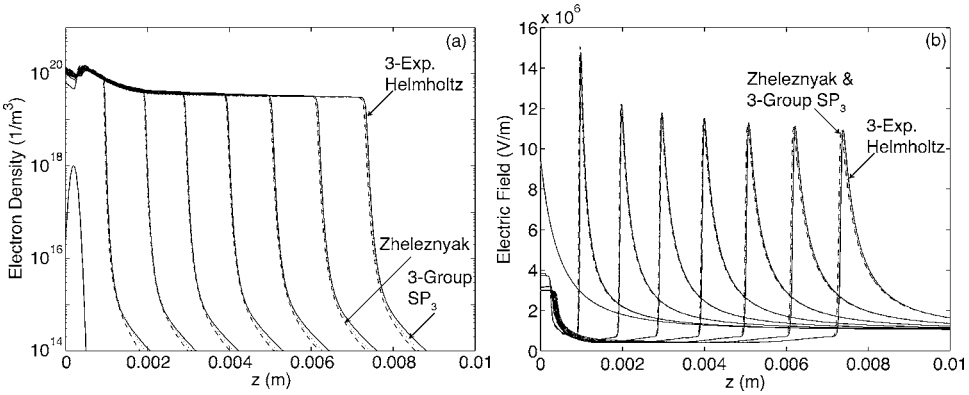

FIG. 3. Same caption as Fig. 2 except that the results are obtained by the Scharfetter-Gummel (SG) based numerical technique (Ref. 1). Dotted line: three-group SP_3 with boundary conditions provided by Zheleznyak integral solution. Dashed line: Zheleznyak model. Solid line: three-exponential Helmholtz model.

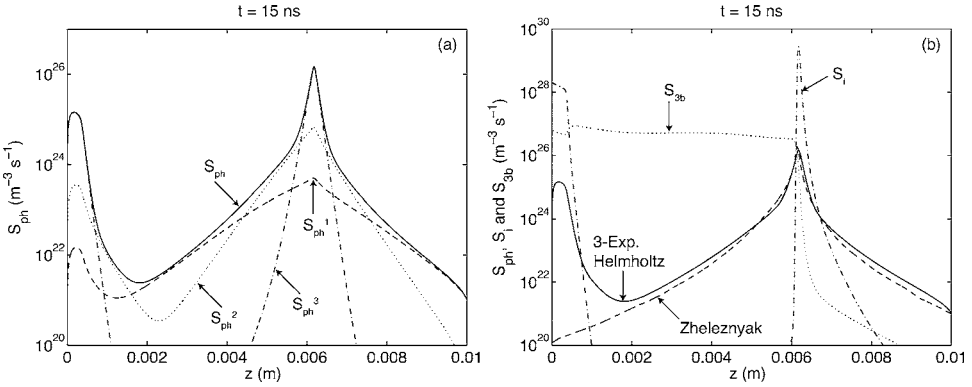

FIG. 4. Photoionization production rate S_{ph} at $t=15$ ns along the symmetry axis of the computational domain. (a) S_{ph} and the three components S_{ph}^1, S_{ph}^2, and S_{ph}^3 of the three-exponential Helmholtz model. (b) S_{ph} calculated using the three-exponential Helmholtz and Zheleznyak models, electron impact ionization production rate S_i, and three-body electron attachment rate S_{3b}.

the streamer [Fig. 1(c)]. These results are notably different from those obtained for a streamer in strong electric field [Fig. 11(c) of Ref. 1], for which significant photoionization is present in the streamer body.

Figure 2 compares the profiles of electron density and the magnitude of the electric field on the symmetry axis of the computational domain calculated using the three-group SP_3 and three-exponential Helmholtz models. The results are shown for the moments of time from $t=0$ to $t=17.5$ ns, with a timestep of 2.5 ns. The results obtained with these two models agree very well in terms of the shape of the profiles, and the magnitudes of the channel density and the peak electric field. For the electron density, only small differences exist in the region well ahead of the streamer head. For the electric field, the difference is almost impossible to notice before 15.0 ns, and relatively small deviations are present at 15.0 and 17.5 ns.

Figure 3 compares the profiles of electron density and the magnitude of the electric field on the symmetry axis of the computational domain calculated using the three-group SP_3 (boundary conditions provided by Zheleznyak integral solution), the three-exponential Helmholtz, and the reference Zheleznyak integral models. An excellent agreement between the results obtained with these three models is observed. Results presented in Figs. 2 and 3 demonstrate that for practical accuracy calculations all three photoionization models (i.e., Zheleznyak, three-group SP_3, and three-exponential Helmholtz) provide adequate and consistent solutions to the streamer problem. Careful inspection of results presented in Figs. 2 and 3 indicates that the modeling results obtained using the SP_3 model are closer to the reference Zheleznyak model results than those obtained with the three-exponential Helmholtz model. The observed better performance of the SP_3 model in comparison with the three-exponential Helmholtz model is consistent with the analysis reported in the appendix of Ref. 1. Furthermore, the possibility of formulating a consistent set of equations and boundary conditions [e.g., Eqs. (1) and (2)] based on radiative transfer physics is a significant advantage of the SP_3 model in comparison with the Helmholtz model.

Figure 4(a) shows the S_{ph} term and the relative distributions of the three components of the three-exponential Helmholtz model on the symmetry axis of the simulation domain at $t=15$ ns. The regions dominated by each component can clearly be identified in the figure. The S_{ph}^1 term, associated with the longest photoionization range,[1] dominates in the region ahead of the streamer head. The S_{ph}^3 term, associated with the shortest photoionization range,[1] is clearly confined to and dominates inside of the streamer head. The S_{ph}^2 term dominates in the intermediate region.

Figure 4(b) compares the photoionization production rate calculated by the three-exponential Helmholtz model and the optimized integral Zheleznyak model, the electron impact ionization rate, and the three-body electron attachment rate. For the photoionization production rate, results from both models are in a very good agreement in the region of, and ahead of the streamer head. A significant difference is observed in the region near the spherical electrode. As discussed in Ref. 1, the optimized integral solution does not include contributions from the emission sources outside of the region around the streamer head, but the Helmholtz solution does. A relatively strong photoionization appears in the region near the spherical electrode implying strong photon emission source in this region. The Helmholtz model automatically accounts for this source when solving the Helmholtz differential equation. The agreement of the modeling results obtained using the two photoionization models shown by Fig. 3 suggests that the different photoionization rates in the region near spherical electrode do not affect the dynamics of the streamer, which is mostly controlled by photons emitted by the streamer head.

Figure 4(b) further indicates that in contrast to the high applied field case, for which electron impact ionization was a dominant process controlling production and loss of electrons in the entire simulation domain (including streamer head and streamer channel regions),[1] the low field case is characterized by the dominance of three-body attachment in the body of the streamer, the dominance of the electron impact ionization in the streamer head, and the dominance of photoionization in the region ahead of the streamer head.

The participation of N. Y. Liu and V. P. Pasko has been supported by the United States National Science Foundation under Grant Nos. NSF ATM-0725360 and ATM-0734083 to Pennsylvania State University.

[1] A. Bourdon, V. P. Pasko, N. Y. Liu, S. Célestin, P. Ségur, and E. Marode, Plasma Sources Sci. Technol. **16**, 656 (2007).
[2] M. B. Zheleznyak, A. Kh. Mnatsakanyan, and S. V. Sizykh, High Temp. **20**, 357 (1982).
[3] G. V. Naidis, Plasma Sources Sci. Technol. **15**, 253 (2006).
[4] A. Luque, U. Ebert, C. Montijn, and W. Hundsdorfer, Appl. Phys. Lett. **90**, 081501 (2007).
[5] P. Ségur, A. Bourdon, E. Marode, D. Bessières, and J. H. Paillol, Plasma Sources Sci. Technol. **15**, 648 (2006).
[6] Y. P. Raizer, *Gas Discharge Physics* (Springer, New York, 1991), p. 135.
[7] N. Y. Liu and V. P. Pasko, J. Phys. D **39**, 327 (2006).
[8] E. W. Larsen, G. Thömmes, A. Klar, M. Seaïd, and T. Götz, J. Comput. Phys. **183**, 652 (2002).